

# Mg<sub>17</sub>Al<sub>12</sub> PHASE PRECIPITATION KINETICS IN DIE CASTING ALLOYS AZ91D AND AM60B

E. A. Payzant, S. R. Agnew, Q. Han and S. Viswanathan

Metals and Ceramics Division  
Oak Ridge National Laboratory  
Oak Ridge, Tennessee 37831

## Abstract

The major second phase in magnesium die casting alloys containing aluminum (i.e., AZ91D and AM60B) is Mg<sub>17</sub>Al<sub>12</sub>, termed  $\beta$ -phase in the magnesium literature. In this study, *in-situ* high temperature x-ray diffraction was used to study the precipitation of this phase from the as-cast matrix. It is indicated that appreciable precipitation of this phase will occur during service at elevated temperatures. Experimental data for the instantaneous volume fraction of  $\beta$ -phase were fit to an adapted Avrami equation. The obtained fit parameters may be used to predict the amount of precipitation that will occur under given service or aging conditions. The impact upon elevated temperature mechanical behavior is also discussed.

**Keywords:** magnesium; die cast; creep; precipitation; alloy development

## 1 Introduction

The automotive industry has renewed interest in magnesium alloys for improving fuel efficiency through vehicle mass reduction. One limitation of magnesium alloys that has hindered more widespread application is their poor creep resistance. The two main die casting alloys are AZ91D and AM60B, which both contain aluminum levels well above the room temperature solid solubility limit (~2%). Recent creep resistant alloy development research has shown that dynamic

precipitation of the Mg<sub>17</sub>Al<sub>12</sub> phase is at least partially responsible for the poor creep behavior of these alloys<sup>1-3</sup>. This motivated a closer examination of Mg<sub>17</sub>Al<sub>12</sub> phase precipitation kinetics.

Table I: Nominal compositions (in wt%) for magnesium alloys AM60B and AZ91D

	AM 60B	AZ 91D
Al	5.7 - 6.3	8.5 - 9.5
Mn	0.27	0.17 - 0.32
Zn	0 - 0.2	0.5 - 0.9
Si	0 - 0.5	0 - 0.2
Cu	0 - 0.008	0 - 0.01
Ni	0 - 0.001	0 - 0.001
Be	0 - 0.001	0 - 0.001
others	0.01 max	0.01 max

## 2 Experimental

*In-situ* high temperature x-ray diffraction was used to investigate  $\beta$ -Mg<sub>17</sub>Al<sub>12</sub> phase precipitation as a function of time and temperature. Data was collected using an automated X-ray powder diffractometer [Model PADX, Scintag Inc., Cupertino, CA] with a Cu normal focus X-ray tube operated at

45 kV and 40 mA and a Si(Li) solid state detector. A Buehler HDK 2.3 high temperature X-ray furnace attachment was operated with a platinum - 30% rhodium resistance strip heater. The samples were studied under a  $1 \times 10^{-5}$  torr vacuum to avoid progressive oxidation

Thin samples (0.5 x 10 x 10 mm) were cut from AM60B (die cast) and AZ91D (permanent mold cast), then polished, etched, and directly fixed to the top surface of the heater strip using carbon paint.

A thermocouple (Type S) was spot-welded to the bottom of the heater strip to measure and control the temperature to a precision of 0.5°C. Accuracy of the temperature is less simple to define, since the surface of such samples is often cooler than the bulk. It also must be noted that the point where the temperature was measured was not the same as the location of the diffracting volume. A temperature of 225°C was chosen for the initial study in order to observe the precipitation reaction within a reasonable amount of time. Sequential 10 minute scans were made over the angular range  $2\theta = 30-50^\circ$  at regular intervals for 30 hours and again at ~48 hours. Subsequent scans were taken on samples at temperatures above and below this value to provide the experimental data for determining the reaction kinetics.

An estimate of the  $\beta$ -phase volume fraction was made from a quantitative Rietveld analysis of the data using the GSAS program<sup>5</sup>, wherein two phases were defined as the hexagonal close-packed solid solution Mg-6%Al (space group P63/mmc) and the cubic  $\beta$ -phase  $Mg_{17}Al_{12}$  (space group I-43m). Finally, the lattice constants of the primary magnesium phase were determined as a function of annealing time. The x-ray diffraction data were analyzed using Jade 5.0 [Materials Data, Inc.] and GSAS [Los Alamos National Laboratory] software.

The refinement strategy in GSAS was to begin with the as-cast pattern and refine the background (3 coefficients), the so-called histogram scale factor (1 coefficient), the lattice parameters of the two phases (1 and 2 coefficients, respectively), and the phase fractions (1 coefficient). The profile parameters and diffractometer constants were established for these samples and experimental conditions and fixed accordingly. For the first pattern at a given temperature, both of the phases' lattice parameters were allowed to be refined, but in subsequent patterns it was found that the lattice parameter of the  $\beta$ -phase  $Mg_{17}Al_{12}$  stayed constant, while that of the h.c.p. matrix changed as the solid solution composition reached its equilibrium value. Thus the refined parameters at time interval  $t$  were used as the starting parameters for the next scan at  $t+1$ , which minimized the time needed to converge to a solution. For the purpose of this investigation, a refined  $\chi^2$  of between 4 and 8 was deemed an acceptable target for estimation of lattice parameters and phase fraction.

### 3 Results

The Mg - Al phase diagram is shown in Figure 1. The compositions of AM60B and AZ91D are marked on this diagram. Although the actual alloys are more complex than simple binaries, the other alloying elements are in very small amounts as shown in Table I. The microstructure of as-cast AM60B (permanent mold) is shown in Figure 2. Since permanent mold gravity casting enforces a much slower cooling rate than die casting, some solid state precipitation of beta phase from supersaturated alpha solid solution occurred,

as indicated by the fine beta platelets surrounding the eutectic beta particle in the center of the micrograph (Fig. 2).

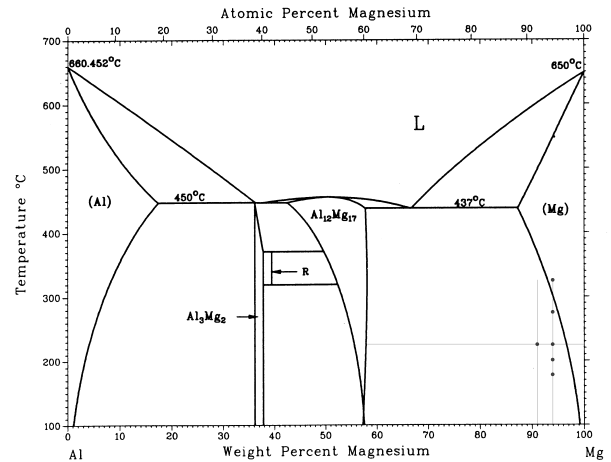


Fig.1. Binary phase diagram for Al-Mg (after reference 4) with nominal compositions indicated by vertical lines and experimental temperatures indicated by solid dots.

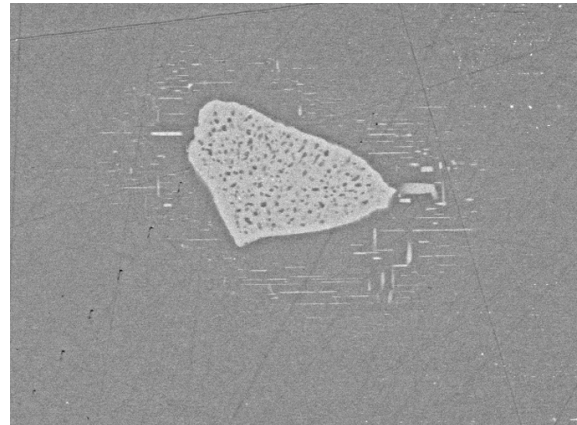


Fig.2. Backscattered electron image of the interdendritic region of the microstructure in permanent mold cast AM60B. The light phase is  $Mg_{17}Al_{12}$  and the dark phase is the Mg solid solution. The large particle represents the as-cast eutectic  $Mg_{17}Al_{12}$  phase, while the small platelets surrounding it are the solid-state transformed  $Mg_{17}Al_{12}$  under investigation.

The AM60B sample showed essentially no preferred orientation or grain size induced anomalies of the peak intensities from a random polycrystal and the two phases could be fit to a high confidence by the Rietveld method as shown in Fig 3. Because the relative X-ray scattering of Al and Mg ions are quite similar, the intensities and phase fractions were insensitive to variations in the Al content of these Mg alloys.

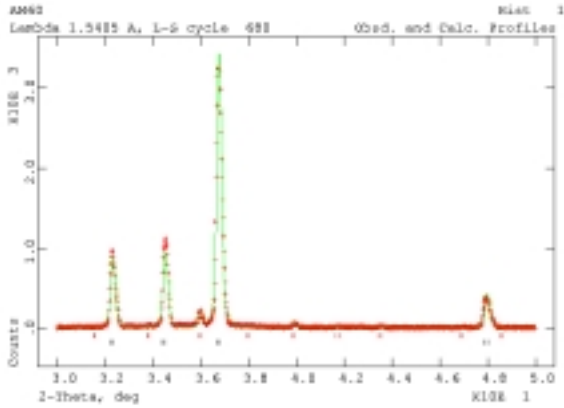


Fig. 3 Plot of typical GSAS refinement of high-temperature X-ray data from an AM60B sample. Over this angular range there are four strong Mg alloy peaks and nine weaker  $\beta$ -phase peaks.

As shown in Figure 4, at 175, 200, and 225 °C the  $\beta$ -phase fraction grew rapidly over the first 3 hours and then leveled off with the characteristic curve one expects of diffusion kinetics, which was least-squares fit by an Avrami equation of the form:

$$\zeta = 1 - \exp(-kt^n) \quad (1)$$

In Figure 5, at a nominal temperature of 250 °C the system rapidly reached equilibrium, and at higher temperatures the  $\beta$ -phase actually decreased with time as in Figure 6, although at a nominal temperature of 275 °C the phase fraction increased over the first 20 minutes before decreasing.

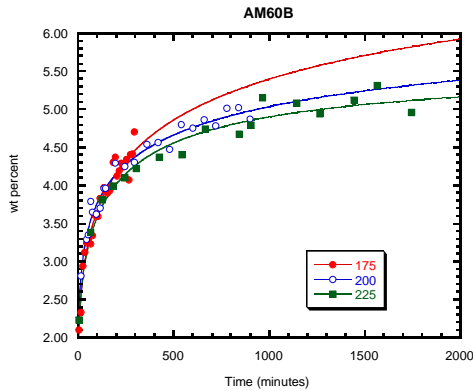


Fig.4 Plot showing increasing phase fraction of  $\beta$ -phase over time for the AM60B sample at nominal temperatures 175, 200 and 225 °C. The superimposed curves are fits to the Avrami equation.

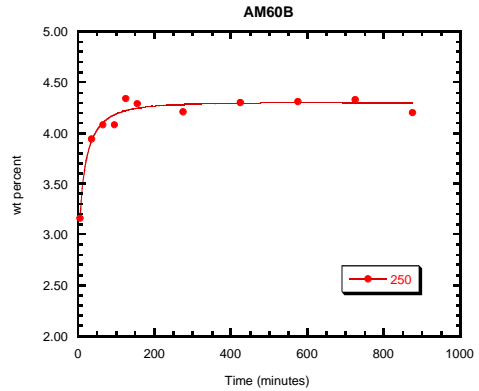


Fig.5 Plot showing constant phase fraction of the  $\beta$ -phase over time for the AM60B sample at a nominal temperature of 250 °C. The superimposed curve is fit to the Avrami equation.

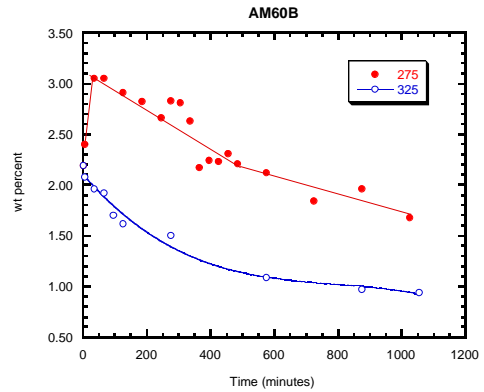


Fig.6 Plot showing decreasing phase fraction of  $\beta$ -phase over time for the AM60B sample at nominal temperatures 275 °C and 325 °C. The curves are not fit to any meaningful equation and are intended as guides to the eye.

#### 4 Discussion

These results make at least qualitative sense when it is recalled that the equilibrium solubility of Al in h.c.p. Mg increases with temperature, as illustrated in Figure 7. At 325 °C one would expect the  $\gamma$ -phase to be completely dissolved into the h.c.p. matrix, but the GSAS refinement indicated the  $\beta$ -phase fraction to level off at less than 1 wt%. This result may illustrate an inability of GSAS to accurately refine extremely low concentrations of a second phase, as a visual analysis could not discern any trace of the  $\beta$ -phase peaks in the pattern.

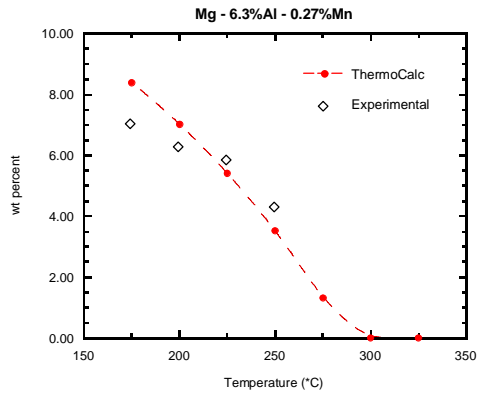


Fig.7 Plot showing the equilibrium  $\beta$ -phase fraction for an AM60B sample as calculated by ThermoCalc. At higher temperatures the amount of  $\beta$ -phase decreases as more Al is soluble in the h.c.p. phase. The experimentally obtained values are superimposed.

As mentioned earlier, the experimental data obtained at 175, 200, 225 and 250°C were fit using an adapted Avrami equation<sup>6</sup>. The time exponent,  $n$ , and rate constant,  $k$ , were obtained from these fits. Since there is a considerable amount of the beta phase present at the start of the experiments, the variable representing time was considered to be in addition to some initial time,  $t_o$ .

$$\frac{f}{f_{eq}} = 1 - \exp[k(t + t_o)^n] \quad (2)$$

In addition, since the as-cast microstructures contain a wide range of compositions, the actual solute concentration which contributes to the local equilibrium beta phase volume fraction is not known *a priori*. Therefore, the equilibrium beta phase volume fraction,  $f_{eq}$ , was also fitted. The ThermoCalc data obtained assuming the nominal composition (Fig. 7) was used as a constant in the above equation to first fit the other 3 parameters:  $t_o$ ,  $k$ , and  $n$ . Then, using the ThermoCalc value as an initial guess,  $f_{eq}$  was allowed to vary as well. The results of this exercise are listed in Table II.

Table II: Fit parameters for the Avrami equation (Eq. 2) obtained from experimental data in Figures 4 and 5.

T (°C)	k	$t_o$ (min)	n	$f_{eq}$
175	0.20	2.6	0.28	7.0
200	0.28	5.5	0.26	6.2
225	0.28	9.6	0.30	5.9
250	0.52	4.3	0.42	4.3

The physical meaning of these parameters in terms of Avrami's original analyses is not clear, since the  $n$  values are much less than 1, while phase transformation problems with 3 dimensional nature typically exhibit  $n = 3$  to 4 and even problems of 1 dimensional nature should have  $n = 1$  to 2 [ref 6]. Given the uncertainties in the determination of  $n$ , all the values listed in Table II are assumed to be essentially

equivalent ( $n \approx 0.3$ ). Similarly, the initial time is also apparently constant ( $t_o \approx 5.5$ ) over the temperature range.

The trends in  $f_{eq}$  and  $k$  are clear, however. In the case of the equilibrium volume fractions, the fitted values are quite close to those we would expect, based on the ThermoCalc equilibrium data plotted in Figure 7. The equilibrium volume fraction of  $\beta$  phase can be interpolated using a linear function of temperature (in °C):

$$f_{eq} = 13 - 0.034T \quad (3)$$

Likewise, the rate constant,  $k$ , increases with increasing temperature and we might expect an Arrhenius type relationship to hold between  $k$  and temperature. However, the scant data prevents determining this relationship with any confidence and, again, linear interpolation is a reasonable approximation within the temperature range of interest:

$$k = -0.51 + 3.9 \times 10^{-3}T \quad (4)$$

Together, these formulae (Eq. 2-4) can be used to predict the degree of beta phase precipitation that would occur as a function of time,  $t$ , at a given temperature (for  $T < 275^\circ\text{C}$ ).

At the highest temperature examined (325°C), the amount of  $\beta$  phase actually decreases towards the equilibrium value (Fig. 6), which at that temperatures is lower than the level initially present in the as-cast material (Fig. 7). At 275°C the most complicated situation is obtained in which the following scenario, presumably, occurs. First the level of beta phase increases as a result of the high level of Al solute found in the interdendritic region. (This may also occur very quickly during the initial phase of the anneal at 325°C.) After the initial increase, equilibrium with the far-field regions of the primary dendrite interiors demands that the level of  $\beta$  phase actually decrease. Since the scenario is significantly more complex than that observed at lower temperatures, and neither service nor aging treatments would require such high temperatures, no fits of these data were attempted.

Unfortunately the AZ91D sample showed significant large grain size and/or preferred orientation anomalies in the peak intensities as compared to a random polycrystal and could not be fit to a high confidence by the Rietveld method. However, monitoring the intensity of the  $\beta$ -phase  $\text{Mg}_{17}\text{Al}_{12}$  provided some measure of the relative changes in the phase fraction of precipitates.

It was also noted that at 225 °C, the lattice parameter of the AZ91D sample took much longer to reach the equilibrium value than for AM60B, as shown in Figure 8. The observed changes in lattice parameter are not the result of thermal expansion, which is instantaneous, or residual strain. Rather, the lattice parameter changes primarily reflect the impact of the Al solid solution atoms on the Mg crystal structure. From the phase diagram one would expect the composition (at least in terms of Al-content), and thus the lattice parameter, of the respective matrix h.c.p. phases to be very nearly identical at this temperature, but the AZ91D lattice volume changes over a period of days whereas AM60B showed little change after the first hour at temperature. This simply implies a greater supersaturation of Al in the Mg matrix in AZ91D than in AM60B.

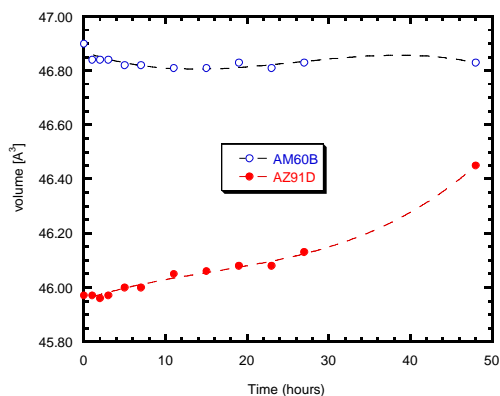


Fig.8 Plot showing evolution of h.c.p. phase atomic volume at a nominal temperature 225 °C for AM60B (top) and AZ91D (bottom). Dashed lines are a guide to the eye.

In a recent study of the tensile and compressive creep behavior of magnesium die casting alloys containing Al, attention was drawn to the changes induced in the Mg matrix lattice parameter as a result of beta phase precipitation<sup>2</sup>. Alloys such as AM60B and AZ91D were shown to creep much faster in tension than in compression at the same nominal applied stress. A connection was drawn between the tension/compression asymmetry and  $\beta$ -phase precipitation. These conclusions were made on the basis of the data such as that plotted in Figure 8. Those data emphasize that as  $\beta$ -phase precipitates, removing Al from solution, the lattice parameters of the surrounding Mg matrix increase. Hence, the amount of  $\beta$ -phase precipitation that occurred during tensile creep was observed to be substantially greater than during compression.

### Summary

Using *in situ* high temperature x-ray diffraction, both as-cast AM60B (die cast) and AZ91D (gravity cast) were shown to precipitate significant volume fractions of  $Mg_{17}Al_{12}$   $\beta$ -phase within the temperature regime of interest (175 - 325 °C). The fine grain size of the die cast AM60B permitted the x-ray diffraction data to be analyzed in a systematic way using the Reitveld analysis of the GSAS code. For temperatures of 250 °C or less, the volume fraction of  $\beta$ -phase grew rapidly during the start of the anneal and then asymptotically approached the equilibrium volume fraction. The volume fractions were fit to an adapted Avrami equation and the obtained fit parameters can be used to predict the amount of precipitation that will occur under given service or aging conditions. At temperatures of 275 °C or more, the as-cast  $\beta$ -phase actually dissolves back into solution.

### Acknowledgements

Research sponsored by the U.S. Department of Energy, Assistant Secretary for Energy Efficiency and Renewable Energy, Office of Transportation Technology, Lightweight Vehicle Materials Program, at ORNL operated by UT-Battelle, LLC, under contract DE-AC05-00OR22725.

### References

1. S. R. Agnew et al., "Tensile and Compressive Creep Behavior of Die Cast Magnesium Alloy AM60B," Magnesium Technology 2000, eds. H. I. Kaplan, J. Hryn, and B. Clow (Warrendale, PA: The Minerals, Metals & Materials Society, 2000) 285-290.
2. M. S. Dargusch, G. L. Dunlop, and K. Pettersen, Magnesium Alloys and Their Applications, eds. B. L. Mordike and K. U. Kainer (Frankfurt, Germany: Werkstoff-Informationsgesellschaft mbH, 1998) 277-282.
3. S. R. Agnew, S. Viswanathan, E. A. Payzant, Q. Han, K. C. Liu, and E. A. Kenik, "Tensile and Compressive Creep Behavior of Magnesium Die Casting Alloys Containing Aluminum," Magnesium Alloys and Their Applications, ed. K. U. Kainer (Weinheim, Germany: Wiley-VCH, 2000) 687-692.
4. T. B. Massalski, ed., Binary Phase Diagrams, vol.1, (Metals Park, OH: The American Society for Metals, 1986) 129-131.
5. A. C. Larson and R. B. von Dreele, GSAS – General Structure Analysis System, LAUR 86-748, Los Alamos, NM 1985
6. J.W. Christian, The Theory of Transformations in Metals and Alloys, 2<sup>nd</sup> edition (Oxford, England: Pergamon Press Ltd., 1975) 15-20